HAL
open science

Quantitative model of Carbon and Nitrogen isotope composition to highlight sources of nutrient discharge in coastal area (Toulon Bay, NW Mediterranean Sea)

Duc Huy Dang, R. Douglas Evans, Gaël Durrieu, Amonda El Houssainy, Jean-Ulrich Mullot, N. Layglon, Véronique Lenoble, Stéphane Mounier, Cédric Garnier

▶ To cite this version:

Duc Huy Dang, R. Douglas Evans, Gaël Durrieu, Amonda El Houssainy, Jean-Ulrich Mullot, et al.. Quantitative model of Carbon and Nitrogen isotope composition to highlight sources of nutrient discharge in coastal area (Toulon Bay, NW Mediterranean Sea). Chemosphere, 2018, 194, pp.543 - 552. 10.1016/j.chemosphere.2017.12.109 . hal-01879413

HAL Id: hal-01879413

https://hal.science/hal-01879413v1

Submitted on 29 Sep 2018

HAL is a multi-disciplinary open access archive for the deposit and dissemination of scientific research documents, whether they are published or not. The documents may come from teaching and research institutions in France or abroad, or from public or private research centers.

L'archive ouverte pluridisciplinaire **HAL**, est destinée au dépôt et à la diffusion de documents scientifiques de niveau recherche, publiés ou non, émanant des établissements d'enseignement et de recherche français ou étrangers, des laboratoires publics ou privés.

*Manuscript
Click here to view linked References

Quantitative model of Carbon and Nitrogen isotope composition to highlight sources of nutrient discharge in coastal sediments (Toulon Bay, NW Mediterranean Sea)

Duc Huy Dang[1,2*], R. Douglas Evans[1,3], Gael Durrieu[2,4], Nicolas Layglon[2], Amonda El Houssainy[2,5], Jean-Ulrich Mullot[6], Véronique Lenoble[2,4], Stéphane Mounier[2,4], Cédric Garnier[2,4]

[1] School of the Environment, Trent University, 1600 West Bank Drive, Peterborough, ON, Canada K9L 0G2

[2] Université de Toulon, PROTEE, EA 3819, CS60584, 83041 Toulon Cedex 9, France

[3] Water Quality Centre, Trent University, 1600 West Bank Drive, Peterborough, ON, Canada K9L 0G2

[4] Université de Toulon, Aix Marseille Université, CNRS, IRD, Mediterranean Institute of Oceanography (MIO), UMR7294, 83041 Toulon Cedex 9, France

[5] Centre National des Sciences Marines, CNRSL, PO Box 534, Batroun, Lebanon

[6] LASEM-Toulon, Base Navale De Toulon, BP 61, 83800 Toulon, France

*Corresponding author. Tel: +1 705 748 1011 (ext. 7692).

E-mail: huydang@trentu.ca

ABSTRACT

Nutrient loadings from either point or non-point sources to the environments are related to the growing global population. Subsequent negative impacts of nutrient loading on the environments requires a better understanding of their biogeochemical cycling and better tools to track their sources. This study examines the C, N and P discharge and cycling in a Mediterranean coastal area from rivers to marine sediments and assesses the anthropogenic contributions. Carbon and N concentrations and isotope compositions in rivers particles, surface sediments, and sediment cores were investigated to build up a quantitative multiple-end-member mixing model for C and N isotopes. This model has allowed determining the contribution of four natural and one anthropogenic sources to the sediments and highlighted the anthropogenic fraction of P based on the relationship with anthropogenic $\delta^{15}N$. Although P is a monoisotopic element and P total concentration has been the sole index to study P loading, this study suggests an alternative approach to differentiate anthropogenic and non-anthropogenic (diagenetic) P and revealed point and non-point sources of P and the corresponding P loading. Also, the diagenetic P background has been established for the 50-cm sediment layer of the whole Bay.

KEYWORDS

Isotope composition; Carbon; Nitrogen; Phosphorus; Coastal area; Point and non-point sources

1. INTRODUCTION

Coastal and estuarine areas are among the most productive, diverse, and economically important ecosystems for human society, and play a primordial role in C and other nutrients storage via primary production. However, these ecosystems are widely and globally threatened, mostly by anthropogenic pressure and impacts of climate change (Hobbie, 2000; Paerl, 2006; UNEP, 2006; Wetz et al., 2008). One of the greatest threats to these ecosystems is eutrophication due to nutrients loading by either point (e.g. waste water discharge) or non-point (e.g. agricultural runoff, atmospheric deposition) sources (Bohlin et al., 2006; Church et al., 2006; Savage et al., 2010; Vaalgamaa et al., 2013) leading to an increasing frequency of harmful algal blooms (Kimbrough et al., 2008; Paerl, 2008, 2006; Vitousek et al., 1997).

Sedimentary accumulation in organic matter (OM) and C-N isotope composition have been used widely as a valuable paleo-environmental tool to track origins of the OM and any change in nutrient availability in surface waters (Bohlin et al., 2006; Church et al., 2006; Di Leonardo et al., 2012; Harmelin-Vivien et al., 2008; Ogrinc et al., 2005; Teranes and Bernasconi, 2000; Vaalgamaa et al., 2013; Yokoyama et al., 2006). The carbon source for terrestrial plants is atmospheric CO_2 with a $\delta^{13}C$ which decreased from -7.5‰ in the 1980s to -8.5‰ today, relative to the Vienna PeeDee Belemnite (Cuntz, 2011). For land vegetation, different assimilation pathways differentiate C3 and C4 plants by typical $\delta^{13}C$ ranges of -24‰ to -34‰ and -10‰ to -20‰, respectively (Dean, 2006; Meyers, 1997). However, most aquatic vegetation obtains its carbon from dissolved inorganic carbon resulting in $\delta^{13}C$ ranging from -18 to -28 ‰ (Bohlin et al., 2006; Dean, 2006; Kendall et al., 2001). The two latter OM pools of terrestrial plants (i.e., land and aquatic) are then indistinguishable by $\delta^{13}C$. However, there is a significant difference in $\delta^{13}C$ between terrestrial and marine organic matter (freshwater and marine phytoplankton: -30 ‰ and 20-22‰, respectively (Bohlin et al., 2006; Bouillon et al., 2012; Meyers, 1997)). Also, among aquatic marine macrophytes, physiological

differences result in variation in $\delta^{13}C$ values in seagrasses and macroalgae (Parker, 1964; Stephenson et al., 1986); a value of -10.5±3.3 ‰ has been reported in 195 observations of seagrasses (Hemminga and Mateo, 1996) while a range from -12 to -18 ‰ is observed for macroalgae (Belicka et al., 2012).

Concerning N, biogeochemical processes tend to enrich ^{15}N leading to a positive drift in $\delta^{15}N$, except for some methanogenic and nitrogen-fixing organisms (e.g., cyanobacteria) (Cloern et al., 2002; Dean, 2006). Relative to atmospheric N_2, $\delta^{15}N$ ranges from +2‰ to +3‰ in soils (Vaalgamaa et al., 2013), and -2‰ to +5‰ in chemical fertilizers (Vaalgamaa et al., 2013) while it ranges between +7‰ to +9‰ in estuarine and marine phytoplankton (Cloern et al., 2002; Vaalgamaa et al., 2013). Also, a peculiarly high value of $\delta^{15}N$ between 10‰ to 25 ‰ is typical of ammonia volatilization in animal manure (Choi et al., 2003) and could be used to track agricultural and urban point sources (e.g., treated/untreated sewage discharge) (Bohlin et al., 2006; Savage et al., 2010; Vaalgamaa et al., 2013). In summary, terrigenous material has lower values in $\delta^{15}N$ and $\delta^{13}C$ than estuarine and marine OM (Ogrinc et al., 2005; Vaalgamaa et al., 2013).

Diverse C-N isotope compositions reflect different sources of the OM. Also, early diagenesis could alter the C-N isotope composition in sediments, mostly by selective degradation of organic compounds and isotope fractionation during degradation (Ogrinc et al., 2005 and references therein). However, this alteration is considered less significant for C (i.e., <2‰) than N (Bohlin et al., 2006; Ogrinc et al., 2005). Nevertheless, contradictory conclusions have been reported for the direction of N isotopic shift during decomposition. It finally appears that the observed change in N isotopic composition (if any) is not related to that in the residual N pool but to the microbially added nitrogen which depends on the N substrate (see discussion in Bouillon et al. (2012) and Lehmann et al. (2002)). This conclusion supports the hypothesis that the vertical variation in C and N isotope composition in sediments could be a useful tool

to track changes in organic matter input (Church et al., 2006; Teranes and Bernasconi, 2000) when diagenetic alterations could be negligible (Engel and Macko, 2013; Kohzu et al., 2011). In addition, eutrophication history could be recorded by C-N isotopes; previous studies (Church et al., 2006; Teranes and Bernasconi, 2000) have reported (i) a significant positive correlation between $\delta^{13}C$ and total sediment P indicating variations in primary production and (ii) a change in sedimentary $\delta^{15}N$ related to an increase in dissolved nitrate, either by algal uptake or a variation in N sources (e.g., wastewater vs. agricultural inputs). However, the diagenetic P cycling is complex; P deposits in sediments in either inorganic or organic forms which are both releasable in porewater due to carrier phase dissolution (e.g., iron oxyhydroxides) and organic matter decomposition, potentially followed by P scavenging via adsorption and/or precipitation processes (Anschutz et al., 2007; Dang et al., 2014a; Krom and Berner, 1981; Ruttenberg, 2003). Therefore, it is not evident to decipher diagenetic P enrichment from anthropogenic P in sediments (Anschutz et al., 2007; Dang et al., 2014b; Ruttenberg, 2003). Unlike C and N, P is a monoisotopic element; it is not possible to track the P sources and biogeochemical processes controlling P cycling by isotope composition.

Globally speaking, the nutrient cycling in coastal areas is challenging due to (i) a multiplicity of sources (several natural and anthropogenic components), (ii) complex biogeochemical processes capable of altering original isotope compositions and (iii) reciprocal interactions with primary production. Resolving this complex system would permit a better evaluation of the contribution from each source and pinpoint human signatures on nutrient inputs to the vulnerable coastal areas. However, although multiples OM sources have been identified in natural coastal sediments, simple mixing models have been used widely with only two end-members as terrestrial and marine materials (Bohlin et al., 2006; Harmelin-Vivien et al., 2008; Li et al., 2016; Loneragan et al., 1997; Ogrinc et al., 2005; Ramaswamy et al., 2008). Scarce are studies on natural sediments with the application of a quantitative multiple-end-member

mixing model (Das et al., 2008). However, stable isotope mixing models using multiple sources have been widely used in food-web studies (see discussion in Erhardt et al. (2014) and Phillips et al. (2014)). This study aims at developing a quantitative multiple-end-member mixing model for C and N isotope composition in the coastal sediments of Toulon Bay (NW Mediterranean Sea) to better highlight anthropogenic contributions to the nutrient balance (either by point or non-point sources) and sedimentary cycling of these nutrients. The proposed model is based on C, N, P, Mg and I concentrations and C, N isotope compositions in several samples of river particles, surface sediments and 50-cm sediment cores at eight stations of the Bay.

2. MATERIALS AND METHODS

2.1. Study site and sampling

Samples were collected in Toulon Bay (Fig. 1, NW Mediterranean, SE French coast), hosting the French Navy Base, yacht clubs, marinas, and aquaculture. Two small urbanized rivers (Las and Eygoutier) and two treated sewage submarine outlets are the main terrestrial/anthropogenic inputs to the sea (point sources), in addition to land runoff (non-point source). The Bay is divided into two non-equal parts, an enclosed western little Bay and a large Bay open to the sea. Previous studies have revealed serious contamination of the entire ecosystem of Toulon Bay, and the situation is more dramatic in little Bay than large Bay (Cossa et al., 2014; Dang et al., 2015a, 2015b, 2014b; Pougnet et al., 2014; Tessier et al., 2011); in little Bay, the seagrass meadow of *Posidonia oceanica* have totally disappeared for the last 30 years, harmful phytoplankton has proliferated, and zooplankton diversity was poor (Bernard et al., 2001; Jamet et al., 2005; Jean et al., 2012).

With the support of the French Navy (boats, materials, divers), undisturbed surface and subsurface sediments (0-5 and 5-10 cm, respectively) were collected from 54 stations situated

141 around the whole Toulon Bay (Fig. 1) using a sediment corer (10-cm diameter and 1-m long
142 Plexiglas tube) that preserved the sediment-water interface (SWI) (Tessier et al., 2011) in
143 December 2008, February and June 2009. In addition, sediment cores (~50 cm long) were
144 collected at eight specific stations (MIS, 3B, LAS1, LAS2, 12, 15, 23 and 52, Fig. 1) during
145 several sampling campaigns from June 2009 to May 2016 (Dang et al., 2015a). Stations
146 LAS1, LAS2 and 23 are situated in front of the two main active tributaries of the Bay (Las
147 and Eygoutier Rivers, Fig. 1) while the former Las river discharged close to station MIS
148 before it was diverted. Stations MIS, 3B and 12 are located in active military zones with
149 intense ship traffic, and station 15 is situated in an aquaculture area (fish and mussel farming).
150 Station 52 is located in large Bay. Sediments were sliced every 2 cm and centrifuged (4000
151 rpm, 15 min, Sigma 3-18K) within 2 h of collection under inert atmosphere (N_2). Pore waters
152 were extracted by filtration of collected supernatants (0.2- m in-line syringe filters, cellulose
153 nitrate, Sartorius) in an N_2-purged glove box.
154 In the two tributaries (Las and Eygoutier Rivers), particles traps were deployed by the IRSN
155 (Radioprotection and Nuclear Safety Institute). Five particle samples were collected in each
156 tributary during a two-week period from October 2012 to May 2013, mostly during rain
157 events (Dang et al., 2015b).
158 All solid fractions were frozen (-18°C) in HDPE bottles, freeze-dried, 2-mm sieved and then
159 kept at -18°C until further treatment.

160 **2.2. Sediment analysis**

161 Total Mg, P and Iodine concentrations were determined by X-Ray Fluorescence (Philips PW
162 2400) equipped with a Rh-tube (detection limit around 0.5%). Particulate organic carbon and
163 total N were analyzed using either a TOC-V_{CSH} analyzer (Shimadzu) or an NCS Flash 2000
164 analyzer (Thermo Scientific). Analytical details and part of the data have been previously

published (Dang et al., 2014a, 2014b; Tessier et al., 2011). Hereafter, C or OC are used for particulate organic carbon.

For C and N stable isotope measurements, sediments were exposed to concentrated HCl vapor for four days to remove the carbonate matrix. Samples of a few mg were then weighted in tin capsules and analyzed at the Water Quality Centre (WQC), Trent University, Canada on a Micromass (Isoprime) Continuous Flow Isotope Ratio Mass Spectrometer (CF-IRMS), equipped with a Eurovector Elemental Analyzer (EA) for sample introduction. Several blanks and certified reference materials (i.e., USGS 40 Glutamic Acid Standard, DG(A1) Glutamic Acid Standard, Casein and High Organic Sediment standard (OAS)) bracketed the samples. A comparison of the analyzed and certified values is shown in Figure S1. The $\delta^{13}C$ and $\delta^{15}N$ isotopic ratios are expressed in the usual δ-notation (part per mil, ‰), relative to Vienna PeeDee Belemnite for C and atmospheric N_2 for N.

2.3. Stable isotope mixing model: IsoSource

IsoSource version 1.3.1 (Phillips et al., 2005; Phillips and Gregg, 2003) was used for source separation, similar to Das et al. (2008). Typically, C and N isotopic composition of several sources are implemented as inputs of different endmembers. For a sediment sample (considered as Mixture), the program determines a range of feasible solutions of source contribution as there are too many combinations to allow a single solution (when the number of sources is higher than the number of used isotope signatures). For n sources S_i, the observed isotopic signature of the Mixture is the sum of products of individual contribution (f_i) and corresponding signature of the source S_i ($\delta^{13}C_i$):

$$\delta^{13}C_{obs} = \sum_{1}^{n} f_i \times \delta^{13}C_i$$

With $\sum_1^n f_i = 1$. Same assumption is made for $\delta^{15}N$.

Examination of relative contributions of each source was performed with small increments (1%) and tolerance (0.1). Individual implemented sources in this study will be detailed in following sections.

3. RESULTS AND DISCUSSION

3.1. C, N and P distribution in sediments

The OC and P profiles at station 3B, 12 and 15 were already shown and discussed previously (Dang et al., 2014b). Averaged concentration in C, N of particles from the two rivers, surface sediments, and sediment cores at eight stations are summarized in Table 1. Concentrations of C and P in surface sediments of the whole Bay are shown in Figure 2. Globally, the C and N profiles are stable all along the core (Dang et al., 2014b) while P profiles, except at station MIS, are stable from the bottom of the core up to -15 cm then increase to the surface (Figure S2). This profile has been reported in other coastal environments (Anschutz et al., 2007; Krom and Berner, 1981) and attributed to either a P loss from sediments to porewater and/or an upward diffusive flux of P which is scavenged in ferric oxyhydroxide precipitates at the SWI (Krom and Berner, 1981; Ruttenberg, 2003). Although the C and P concentrations in surface sediments at the scale of the Bay average ca. 3.9 ±1.5 % and 530 ±150 g g^{-1} (Table 1), some hot spots in C and P can be noticed: northern parts of little Bay, the aquaculture area (station 15), and the two outlets of treated sewage (Figure 2) which could suggest there is non-point (land runoff) and point (aquaculture, sewage outlet) sources in the Bay. However, a possibility of stronger diagenetic activities at these locations leading to stronger P accumulation could not be excluded. Also, such surface mapping seems to show a dilution effect of the Las River particles to the sediment in the north of the Little Bay (Fig. 2); as particles transported in the Las River consisted of low C, N and P (0.9 %, 0.07 % and 410 g

g^{-1}, respectively), lower than that of the Eygoutier River (3 %, 0.21 % and 1240 g g^{-1}, respectively). Although the two watersheds are karstic, Eygoutier River takes it source from an agricultural area, when the Dardennes dam upstream in the Las should hold back significantly on particle discharge (Dufresne, 2014; Nicolau et al., 2012). These peculiarities should explain the difference between the contents of C, N and P in the two rivers.

Also, particles from the 2 rivers have similar C/N ratios (*ca.* 14.2 g g^{-1}) and surface and sediment cores presented higher values in C/N ratio (up to 44.9 g g^{-1}, Fig. 3A). Even when considering a potential contribution of marine plankton (C/N ratio of 6.6, (Redfield et al., 1963)), such increase in C/N ratio in sediments compared to sources (terrestrial particles and/or marine planktons) could be due to the diagenetic preferential degradation of N-rich compounds (Burdige, 2007; Hammond et al., 1999). In fact, a previous study has shown that the C/N ratio in porewaters at station 12 was 8.6 (g g^{-1}, r^2=0.9, n = 275) (Dang et al., 2014a) when the C/N ratio observed in station-12 sediments was 18.6 g g^{-1} (Figure 3A). Compared to the C/N ratio of the river particles of 14.2 g g^{-1} (Figure 3A), this observation confirms the diagenetic degradation of N-rich compounds leading to an N-depletion in sediments and N-enrichment in porewater. Moreover, it seems that the C and N mass balance is preserved between the residual C and N in sediments and the biologically released C and N in porewater. This makes the C/N ratio a non-suitable index to track OM source in marine sediments, except when it is correctly balanced. Similarly for the C and P relationship, the C/P ratio in river particles is *ca.* 25.7 g g^{-1} and a P-depletion is observed in sediments (up to 116.7 g g^{-1} excluding station 15, Fig. 3B).

3.2. C and N isotope composition

Vertical profiles of $\delta^{13}C$ and $\delta^{15}N$ in river particulate matter and in sediments at eight stations are summarized in Figure S3. Despite the difference in C and N concentration in particles of

the two rivers, C and N isotope compositions are similar with values of $\delta^{13}C$ and $\delta^{15}N$ of -28.5 ‰ and 5.0 ‰, respectively (Table 1). The $\delta^{13}C$ profiles in sediment cores were uniformly stable; the standard deviation being less than 10% of the average value (Figure S3 A, B, Table 1). The $\delta^{13}C$ average ranges from -30.1 to -15.8 ‰ with the most negative values observed at stations MIS, LAS1 and LAS2, probably due to the impact of the delivered particles. In these three sediment cores, $\delta^{15}N$ profiles were among the most stable while other sediments cores showed a clear ^{15}N depletion profile from the top to the bottom of the core (Figure S3 C, D).

By gathering paired values of $\delta^{13}C$ and $\delta^{15}N$ from the literature on C and N isotope composition in coastal areas (Table S1 and Figure S4), three main zones including freshwater phytoplankton, estuarine-marine phytoplankton and macroalgae/seagrasses (Figure S4) cover most of the $\delta^{13}C$-$\delta^{15}N$ biplot in the Toulon Bay sediments (Figure 4). However, within the C and N isotope signature of macroalgae/seagrasses, several studies have shown that some macroalgae were more depleted in ^{13}C than seagrasses, probably due to the physiological morphology and the C uptake mechanisms (Alomar et al., 2016; Hemminga and Mateo, 1996; Jennings et al., 1997; Stephenson et al., 1986). Therefore, while compared to the data in the Toulon Bay, we have divided the macroalgae/seagrasses group into an additional fourth group containing solely ^{13}C- and ^{15}N-depleted values reported for macroalgae (Table S1, Figure S4). Consequently, four natural sources are compiled from the literature (i) S1: freshwater phytoplankton, (ii) S2: estuarine-marine phytoplankton, (iii) S3: seagrasses/macroalgae and (iv) S4: macroalgae. In addition, one anthropogenic source (Source A) could be implemented. For that, at stations MIS, 3B, 12, 15 and 23, a significant correlation between $\delta^{13}C$ and P is observed ($n = 28$, $r^2 = 0.71$, $p < 0.0001$) reveals that such high accumulation in P (up to 1400 g g^{-1} at station MIS) could be an anthropogenic input in the area, together with a specific signature of C. The corresponding $\delta^{13}C$ of the source A was then assumed to that of the

sample the most concentrated in P ($\delta^{13}C_{sourceA}$ = -26.5 ‰). The $\delta^{15}N_{sourceA}$ was assumed to be 10 ‰, as usually found for anthropogenic N isotope composition from urban and aquaculture impacts (Savage et al., 2010; Yokoyama et al., 2006). These five sources (Figure 4) have been utilized in the IsoSource program to calculate the respective contribution of each individual source to the observed C and N isotope composition in Toulon Bay sediments.

3.3. A quantitative multiple-endmember mixing model for C and N isotope composition

Outputs of the IsoSource model are relative contributions of each of five sources previously defined. The modeled C and N isotope composition is compared to that observed in sediments (Figure 5). For C, the model has calculated well the isotope composition of all sediments (Figure 5A). However, the model has predicted well for only 80 percent of the dataset of N and there is an offset of 1.15 ‰ concerning 20 % of the samples having the largest contributions of Source 4 (Figure 5B). This includes the samples the most depleted in ^{15}N. The offset of 1.15 ‰ falls within the error of the source 4 ($\delta^{15}N_{Source4}$ = 1.5±1.2 ‰) and the difference between the average (1.5‰) and the most depleted value recorded in our sediments (Figure 4). Other studies have already reported *Caulerpa sp.*, the most important invasive macroalgae in the Mediterranean Sea (Alomar et al., 2016), with such depletion in ^{15}N ($\delta^{15}N$ = 0.3±0.43 ‰ to 1.7±0.56%) and a similar composition in C ($\delta^{13}C$ = -23±0.51 ‰ to -20.1±0.26%) to our sediments (Loneragan et al., 1997). However, without a confirmation of the isotopic composition of macroalgae populations in Toulon Bay, the averaged isotope composition of Source4 is not shifted assuming that the model for N isotope is still considered correct (slope = 1.03, r^2 = 0.79, Figure 5B) and taking into account analytical and modeling errors. Also, this model did not take into account stations LAS1 and LAS2 as their C and N isotopic composition did not fall in the zone defined by the five sources. That would require an additional source depleted in both ^{13}C and ^{15}N (Figure 4). Such situation has been reported

for a coastal wetland ($\delta^{15}N$ = 0.7±0.8 ‰ and $\delta^{13}C$ -26.8±1% (Li et al., 2016)). Nevertheless, without having investigated in the signature of the Toulon Bay "urban" wetland, this firth natural source is not added in the model.

Contributions of each of the five sources to the C and N isotope composition in six sediments cores are summarized in radar plots (Figure 6). For station MIS, sources 1 and 4 are dominant while at the station 3B, C and N isotope compositions are predicted to be from all five sources with a slightly higher contribution from source 2. Stations 12 and 15 are similar, with a strong contribution of source 3. From land to sea, the contribution of Source 4 increases from land to sea to reach equal contribution with Source 3 at station 23, and dominant contribution at station 52. In summary, there is a transition of the relative source contributions from the coast to the open part of the Bay (i.e., from station MIS to 52). Station MIS which is the most northern in little Bay is strongly influenced by the terrestrial input (Source 1). Station 3B which is situated in a zone where macrophytes are devastated has equal contributions from all sources with a slight dominance of marine phytoplankton signature (Source 2). Stations 12 and 15 are located in a shallow water-column zone and have a strong seagrass signature (Source 3). In the large Bay, C and N isotope compositions seemed to be depleted in ^{15}N which can result from the presence of macroalgae (Source 4). However, as concentrations in C and N at these stations are lower than other stations, the influence of diagenetic alteration on C and N isotope composition could be more significant than for the rest of the Bay.

As the anthropogenic contribution could be from either non-point (runoff) or point (treated sewage) sources, contributions of Source 1 (terrestrial input) and Source A (Anthropogenic source) were used to evaluate the anthropogenic signature of N isotope composition ($\delta^{15}N_{anthr.}$):

$$\delta^{15}N_{anthr.} = f_{source1} \times \delta^{15}N_{source1} + f_{sourceA} \times \delta^{15}N_{sourceA}$$

For stations where these sources are recurrent, this calculation revealed a significant relationship between total P and $\delta^{15}N_{anthr.}$ rather than $\delta^{15}N_{bulk}$ (Figure 7); this P-$\delta^{15}N_{anthr.}$ relationship involves stations MIS, 3B and 12, demonstrating a potential co-contamination of P and anthropogenic N in the northern part of the Bay. On the other hand, when comparing total P to total I and Mg in sediments of the whole system (Figure 8), strong relationships are observed among them, only at stations 15, 23 and 52 but not for those where P is correlated to $\delta^{15}N_{anthr.}$ (i.e., MIS, 3B and 12). In fact, Iodine is released in sediment porewater as an organic matter decomposition product in anoxic conditions, then converted into solid phases in oxic conditions due to the affinity to iron oxyhydroxide (Gao et al., 2003; Ullman and Aller, 1980; Xianhao et al., 1992). Similar diagenetic behavior is stated for P (Ruttenberg, 2003). In addition, there is a negative correlation between Mg and P at stations 15, 23 and 52 (Figure 8B), which confirms once again that P accumulation in these stations is related to diagenetic processes as Mg is accumulated by carbonate mineral precipitation where CO_2 is released from organic carbon oxidation (Metzger et al., 2007). The correlation between Iodine, Mg and P in sediments at station 15, 23 and 52 (Figure 8) supports the hypothesis that diagenetic reactions are the major processes leading to P accumulation at these stations but not an additional anthropogenic input. These approaches (as shown in Figures 7 and 8) allow us to differentiate the anthropogenic and "non-anthropogenic/diagenetic" pools of P in coastal sediments.

Eventually, applying the multiple end-member mixing model for C and N and the relationship to P for the surface sediments of the whole Toulon Bay ($P_{anthr.} = 270 \times \delta^{15}N_{anthr.}$, Figure 7), surface (0-5 cm) distribution of anthropogenic P was calculated (Figure 9). This revealed a non-point source with strong P loading in the northern part of the little Bay and several point

330 sources at stations 15 (aquaculture area), 39 and 42 (treated sewage outlet). This supports not
331 only the validity of the model but also the applicability of the approach to detecting
332 anthropogenic P loading in coastal sediments. This approach seems to be more refined than
333 using total OC and/or P as shown in Figure 2.
334 In addition, the non-anthropogenic P is calculated as the difference between total P and $P_{anthr.}$
335 in six sediments cores (Figure 10). The applied model allowed us to assess the background of
336 P in the Bay and revealed P accumulation only by diagenetic reactions just below the SWI.
337 Indeed, from various profiles of total P in several sediments cores within the Bay (range of
338 300-2000 g g^{-1}, Figure S2), the non-anthropogenic P profiles for six stations were identical
339 (Figure 10A) with a typical stable background P concentration of 350±60 (2sd) g g^{-1} and an
340 diagenetic accumulation leading up to 60 % of the P background concentration at the top
341 sediment layer (Figure 10B).
342
343 **4. CONCLUSIONS**
344 C and N isotope ratios have been proven to be useful proxies to (i) decode biogeochemical
345 processes involving the organic matter, (ii) to study the food web and (iii) to assess ecological
346 impacts in a changing world. However, relatively few studies exist that have developed
347 quantitative mixing models for C and N isotopes with multiple sources taken into account.
348 This study has shown:
349 - The applicability of such quantitative multiple end-member mixing models for C and N
350 isotopes to track organic matter and nutrient sources in coastal environments.
351 - The possibility to differentiate anthropogenic N and P from diagenetic accumulation ("non-
352 anthropogenic").

- An estimate of point and non-point sources of P in the coastal area of Toulon Bay (runoff and aquaculture-treated sewage, respectively).

- An evaluation of the sedimentary P background profile for the whole Bay of Toulon.

ACKNOWLEDGEMENTS:

This study was part of the MerMex-MERITE/MISTRALS research program (part of the international IMBER, LOICZ, and SOLAS projects), and funded through the CARTOCHIM, CARTOC, PREVENT and METFLUX research programs (funded by "Toulon-Provence-Méditerranée (TPM)", the "Région PACA", the "Conseil Départemental du Var" and "l'Agence de l'Eau Rhône-Méditerranée et Corse"). DHD's Ph.D. and postdoctoral fellowships were respectively supported by the French Ministry of National Education, Higher Education and Research and a Canadian NSERC (Natural Sciences and Engineering Research Council) Collaborative Research and Development Grant to RDE, which also funded the analyses carried out at the Trent WQC. The authors wish to thank the French Navy for diving and sampling assistance, Dr. Jean-Francois Koprivnjak for isotope measurements.

REFERENCES

Alomar, C., Deudero, S., Andaloro, F., Castriota, L., Consoli, P., Falautano, M., Sinopoli, M., 2016. Caulerpa cylindracea Sonder invasion modifies trophic niche in infralittoral rocky benthic community. Mar. Environ. Res. 120, 86–92. doi:10.1016/j.marenvres.2016.07.010

Anschutz, P., Chaillou, G., Lecroart, P., 2007. Phosphorus diagenesis in sediment of the Thau Lagoon. Estuar. Coast. Shelf Sci. 72, 447–456. doi:10.1016/j.ecss.2006.11.012

Belicka, L.L., Burkholder, D., Fourqurean, J.W., Heithaus, M.R., MacKo, S.A., Jaff́, R., 2012. Stable isotope and fatty acid biomarkers of seagrass, epiphytic, and algal organic matter to consumers in a pristine seagrass ecosystem. Mar. Freshw. Res. 63, 1085–1097. doi:10.1071/MF12027

Bernard, G., Denis, J., Deneux, F., Belsher, T., Sauzade, D., Boudouresque, C.F., Charbonnel, E., Emery, E., Herve, G., Bonhomme, P., 2001. Etude et cartographie des biocénoses de la rade de Toulon, in: Contrat D'étude Pour Le Syndicat Intercommunal de l'Aire Toulonaise, Ifremer et GISPosidonie. Ifremer Publ, La Seyne, p. 150.

Bohlin, H.S., Mörth, C.M., Holm, N.G., 2006. Point source influences on the carbon and nitrogen geochemistry of sediments in the Stockholm inner archipelago, Sweden. Sci. Total Environ. 366, 337–349. doi:10.1016/j.scitotenv.2005.07.016

Bouillon, S., Connolly, R.M., Gillikin, D.P., 2012. Use of Stable Isotopes to Understand Food Webs and Ecosystem Functioning in Estuaries, Treatise on Estuarine and Coastal Science. Elsevier Inc. doi:10.1016/B978-0-12-374711-2.00711-7

Burdige, D.J., 2007. Preservation of organic matter in marine sediments: controls, mechanisms, and an imbalance in sediment organic carbon budgets? Chem. Rev. 107, 467–85. doi:10.1021/cr050347q

Choi, W.J., Lee, S.M., Ro, H.M., 2003. Evaluation of contamination sources of groundwater NO 3− using nitrogen isotope data: A review. Geosci. J. 7, 81–87.

Church, T.M., Sommerfield, C.K., Velinsky, D.J., Point, D., Benoit, C., Amouroux, D., Plaa, D., Donard, O.F.X., 2006. Marsh sediments as records of sedimentation, eutrophication and metal pollution in the urban Delaware Estuary. Mar. Chem. 102, 72–95. doi:10.1016/j.marchem.2005.10.026

Cloern, J., Canuel, E., Harris, D., 2002. Stable carbon and nitrogen isotope composition of aquatic and terrestrial plants of the San Francisco Bay estuarine system. Limnol. Oceanogr. 47, 713–729.

Cossa, D., Garnier, C., Buscail, R., Elbaz-Poulichet, F., Mikac, N., Patel-Sorrentino, N., Tessier, E., Rigaud, S., Lenoble, V., Gobeil, C., 2014. A Michaelis–Menten type equation for describing methylmercury dependence on inorganic mercury in aquatic sediments. Biogeochemistry 119, 35–43. doi:10.1007/s10533-013-9924-3

Cuntz, M., 2011. Carbon cycle: A dent in carbon's gold standard. Nature 477, 547–548. doi:10.1038/477547a

Dang, D.H., Lenoble, V., Durrieu, G., Mullot, J.-U., Mounier, S., Garnier, C., 2014a.

Sedimentary dynamics of coastal organic matter: An assessment of the porewater size/reactivity model by spectroscopic techniques. Estuar. Coast. Shelf Sci. 151, 100–111. doi:10.1016/j.ecss.2014.10.002

Dang, D.H., Lenoble, V., Durrieu, G., Omanović, D., Mullot, J.-U., Mounier, S., Garnier, C., 2015a. Seasonal variations of coastal sedimentary trace metals cycling: Insight on the effect of manganese and iron (oxy)hydroxides, sulphide and organic matter. Mar. Pollut. Bull. 92, 113–124. doi:10.1016/j.marpolbul.2014.12.048

Dang, D.H., Schaefer, J., Brach-Papa, C., Lenoble, V., Durrieu, G., Dutruch, L., Chiffoleau, J.-F., Gonzalez, J.-L., Blanc, G., Mullot, J.U., Mounier, S., Garnier, C., 2015b. Evidencing the impact of coastal contaminated sediments on mussels through Pb stable isotopes composition. Environ. Sci. Technol. 49, 11438–11448. doi:10.1021/acs.est.5b01893

Dang, D.H., Tessier, E., Lenoble, V., Durrieu, G., Omanović, D., Mullot, J.-U., Pfeifer, H.-R., Mounier, S., Garnier, C., 2014b. Key parameters controlling arsenic dynamics in coastal sediments: an analytical and modeling approach. Mar. Chem. 161, 34–46.

Das, B., Nordin, R., Mazumder, A., 2008. An alternative approach to reconstructing organic matter accumulation with contrasting watershed disturbance histories from lake sediments. Environ. Pollut. 155, 117–124. doi:10.1016/j.envpol.2007.10.031

Dean, W.E., 2006. Characterization of Organic Matter in Lake Sediments from Minnesota and Yellowstone National Park, U.S. Geological Survey Open-File Report 2006-1053.

Di Leonardo, R., Cundy, A.B., Bellanca, A., Mazzola, A., Vizzini, S., 2012. Biogeochemical evaluation of historical sediment contamination in the Gulf of Palermo (NW Sicily): Analysis of pseudo-trace elements and stable isotope signals. J. Mar. Syst. 94, 185–196. doi:10.1016/j.jmarsys.2011.11.022

Dufresne, C., 2014. Compréhension et analyse des processus hydrosédimentaires dans la baie de Toulon. Apport à la modélisation de la dispersion des radionucléides. Université de Toulon.

Engel, M., Macko, S.A., 2013. Organic Geochemistry: Principles and Applications. Springer Science & Business Media.

Erhardt, E.B., Wolf, B.O., Ben-David, M., Bedrick, E.J., 2014. Stable Isotope Sourcing Using Sampling. Open J. Ecol. 4, 289–298. doi:10.4236/oje.2014.46027

Gao, A.G., Liu, Y.G., Zhang, D.J., Sun, H.Q., 2003. Latitudinal distribution of iodine in sediments in the Chukchi Sea and the Bering Sea. Sci. China Ser. D-Earth Sci. 46, 592–602. doi:10.1360/03yd9052

Hammond, D.E., Giordani, P., Berelson, W.M., Poletti, R., 1999. Diagenesis of carbon and nutrients and benthic exchange in sediments of the Northern Adriatic Sea. Mar. Chem. 53–79.

Harmelin-Vivien, M., Loizeau, V., Mellon, C., Beker, B., Arlhac, D., Bodiguel, X., Ferraton, F., Hermand, R., Philippon, X., Salen-Picard, C., 2008. Comparison of C and N stable isotope ratios between surface particulate organic matter and microphytoplankton in the Gulf of Lions (NW Mediterranean). Cont. Shelf Res. 28, 1911–1919. doi:10.1016/j.csr.2008.03.002

Hemminga, M.A., Mateo, M.A., 1996. Stable carbon isotopes in seagrasses: Variability in ratios and use in ecological studies. Mar. Ecol. Prog. Ser. 140, 285–298. doi:10.3354/meps140285

Hobbie, J.E., 2000. Estuarine Science: A Synthetic Approach to Research and Practice. Washington, DC.

Jamet, J.L., Jean, N., Bogé, G., Richard, S., Jamet, D., 2005. Plankton succession and assemblage structure in two neighbouring littoral ecosystems in the north-west Mediterranean Sea. Mar. Freshw. Res. 56, 69–83. doi:10.1071/MF04102

Jean, N., Dumont, E., Durrieu, G., Balliau, T., Jamet, J.-L., Personnic, S., Garnier, C., 2012. Protein expression from zooplankton communities in a metal contaminated NW mediterranean coastal ecosystem. Mar. Environ. Res. 80, 12–26. doi:10.1016/j.marenvres.2012.06.004

Jennings, S., Reñones, O., Morales-Nin, B., Polunin, N.V.C., Moranta, J., Coll, J., 1997. Spatial variation in the 15N and 13C stable isotope composition of plants, invertebrates and fishes on Mediterranean reefs: Implications for the study of trophic pathways. Mar. Ecol. Prog. Ser. 146, 109–116. doi:10.3354/meps146109

Kendall, C., Silva, S.R., Kelly, V.J., 2001. Carbon and nitrogen isotopic compositions of particulate organic matter in four large river systems across the United States. Hydrol. Process. 15, 1301–1346. doi:10.1002/hyp.216

Kimbrough, K.L., Johnson, W.E., Lauenstein, G.G., Chrstensen, J.D., Apeti, D.A., 2008. An assessment of two decades of contaminant monitoring in the nation's coastal zone. Silver Spring, MD. NOAA Technical Memorandum NOS NCCOS 74. Silver Spring, MD.

Kohzu, A., Imai, A., Ohkouchi, N., Fukushima, T., Kamiya, K., Komatsu, K., Tomioka, N., Kawasaki, N., Miura, S., Satou, T., 2011. Direct evidence for the alteration of 13C natural abundances during early diagenesis in Lake Kasumigaura, Japan. Geochemistry, Geophys. Geosystems 12, 1–14. doi:10.1029/2011GC003532

Krom, M.D., Berner, R.A., 1981. The diagenesis of phosphorus in a nearshore marine sediment. Geochim. Cosmochim. Acta 45, 207–216. doi:10.1016/0016-7037(81)90164-2

Lehmann, M., Bernasconi, S., Barbieri, A., McKenzie, J., 2002. Preservation of organic matter and alteration of its carbon and nitrogen isotope composition during simulated and in situ early sedimentary diagenesis. Geochim. Cosmochim. Acta 66, 3573–3584. doi:10.1016/S0016-7037(02)00968-7

Li, Y., Zhang, H., Tu, C., Fu, C., Xue, Y., Luo, Y., 2016. Sources and fate of organic carbon and nitrogen from land to ocean: Identified by coupling stable isotopes with C/N ratio. Estuar. Coast. Shelf Sci. 181, 114–122. doi:10.1016/j.ecss.2016.08.024

Loneragan, N.R., Bunn, S.E., Kellaway, D.M., 1997. Are mangroves and seagrasses sources of organic carbon for penaeid prawns in a tropical Australian estuary? A multiple stable-isotope study. Mar. Biol. 130, 289–300. doi:10.1007/s002270050248

Metzger, E., Simonucci, C., Viollier, E., Sarazin, G., Prévot, F., Jézéquel, D., 2007. Benthic response to shellfish farming in Thau lagoon: Pore water signature. Estuar. Coast. Shelf Sci. 72, 406–419. doi:10.1016/j.ecss.2006.11.011

Meyers, P.A., 1997. Organic geochemical proxies of paleoceanographic, plaeolimnologic, and plaeoclimatic processes. Org. Geochem. 27, 213–250.

Nicolau, R., Lucas, Y., Merdy, P., Raynaud, M., 2012. Base flow and stormwater net fluxes of carbon and trace metals to the Mediterranean sea by an urbanized small river. Water

Res. 46, 6625–6637. doi:10.1016/j.watres.2012.01.031

Ogrinc, N., Fontolan, G., Faganeli, J., Covelli, S., 2005. Carbon and nitrogen isotope compositions of organic matter in coastal marine sediments (the Gulf of Trieste, N Adriatic Sea): Indicators of sources and preservation. Mar. Chem. 95, 163–181. doi:10.1016/j.marchem.2004.09.003

Paerl, H., 2008. Nutrient and other environmental controls of harmful cyanobacterial blooms along the freshwater-marine continuum. Adv. Exp. Med. Biol. 619, 217–37. doi:10.1007/978-0-387-75865-7_10

Paerl, H.W., 2006. Assessing and managing nutrient-enhanced eutrophication in estuarine and coastal waters: Interactive effects of human and climatic perturbations. Ecol. Eng. 26, 40–54. doi:10.1016/j.ecoleng.2005.09.006

Parker, P., 1964. The biogeochemistry of the stable isotopes of carbon in a marine bay. Geochim. Cosmochim. Acta 28, 1155–1164. doi:10.1016/0016-7037(64)90067-5

Phillips, D.L., Gregg, J.W., 2003. Source partitioning using stable isotopes: Coping with too many sources. Oecologia 136, 261–269. doi:10.1007/s00442-003-1218-3

Phillips, D.L., Inger, R., Bearhop, S., Jackson, A.L., Moore, J.W., Parnell, A.C., Semmens, B.X., Ward, E.J., 2014. Best practices for use of stable isotope mixing models in food-web studies. Can. J. Zool. 835, 823–835.

Phillips, D.L., Newsome, S.D., Gregg, J.W., 2005. Combining sources in stable isotope mixing models: Alternative methods. Oecologia 144, 520–527. doi:10.1007/s00442-004-1816-8

Pougnet, F., Schäfer, J., Dutruch, L., Garnier, C., Tessier, E., Dang, D.H., Lanceleur, L., Mullot, J.-U., Lenoble, V., Blanc, G., 2014. Sources and historical record of tin and butyl-tin species in a Mediterranean bay (Toulon Bay, France). Environ. Sci. Pollut. Res. Int. 21, 6640–51. doi:10.1007/s11356-014-2576-6

Ramaswamy, V., Gaye, B., Shirodkar, P. V., Rao, P.S., Chivas, A.R., Wheeler, D., Thwin, S., 2008. Distribution and sources of organic carbon, nitrogen and their isotopic signatures in sediments from the Ayeyarwady (Irrawaddy) continental shelf, northern Andaman Sea. Mar. Chem. 111, 137–150. doi:10.1016/j.marchem.2008.04.006

Redfield, A.C., Ketchum, B.H., Richards, F.A., 1963. The Influence of Organisms on the Composition of Sea Water. Sea.

Ruttenberg, K.C., 2003. The Global phosphorus cycle, in: Turekian, K.K., Holland, H.D. (Eds.), Treatise on Geochemistry. Elsevier Ltd, pp. 585–643.

Savage, C., Leavitt, P.R., Elmgren, R., 2010. Effects of land use, urbanization, and climate variability on coastal eutrophication in the Baltic Sea. Limnol. Oceanogr. 55, 1033–1046. doi:10.4319/lo.2010.55.3.1033

Stephenson, R., Tan, F., Mann, K., 1986. Use of stable carbon isotope ratios to compare plant material and potential consumers in a seagrass bed and a kelp bed in Nova Scotia, Canada. Mar. Ecol. Prog. Ser. 30, 1–7. doi:10.3354/meps030001

Teranes, J.L., Bernasconi, S.M., 2000. The record of nitrate utilization and productivity limitation provided by d15N values in lake organic matter—. A study of sediment trap and core sediments from Baldeggersee, Switzerland. Limnol. Oceanogr. 45, 801–813. doi:10.4319/lo.2000.45.4.0801

Tessier, E., Garnier, C., Mullot, J.-U., Lenoble, V., Arnaud, M., Raynaud, M., Mounier, S., 2011. Study of the spatial and historical distribution of sediment inorganic contamination in the Toulon bay (France). Mar. Pollut. Bull. 62, 2075–2086. doi:10.1016/j.marpolbul.2011.07.022

Ullman, W.J., Aller, R.C., 1980. Dissolved iodine flux from estuarine sediments and implications for the enrichment of iodine at the sediment water interface. Geochim. Cosmochim. Acta 44, 1177–1184. doi:10.1016/0016-7037(80)90071-X

UNEP, 2006. Marine and coastal ecosystem and human well-being: A synthesis report based on the findings of the Millennium Ecosystem Assessment.

Vaalgamaa, S., Sonninen, E., Korhola, A., Weckström, K., 2013. Identifying recent sources of organic matter enrichment and eutrophication trends at coastal sites using stable nitrogen and carbon isotope ratios in sediment cores. J. Paleolimnol. 50, 191–206. doi:10.1007/s10933-013-9713-y

Vitousek, P.M., Mooney, H. a, Lubchenco, J., Melillo, J.M., 1997. Human Domination of Earth' s Ecosystems. Science (80-.). 277, 494–499. doi:10.1126/science.277.5325.494

Wetz, M.S., Hales, B., Wheeler, P.A., 2008. Degradation of phytoplankton-derived organic matter: Implications for carbon and nitrogen biogeochemistry in coastal ecosystems. Estuar. Coast. Shelf Sci. 77, 422–432. doi:10.1016/j.ecss.2007.10.002

Xianhao, C., Weiping, X., Haisheng, Z., 1992. Remobilization and accumulation of iodine in marine sediments, Western Antartic ocean. Antarct. Res. 3, 50–59.

Yokoyama, H., Abo, K., Ishihi, Y., 2006. Quantifying aquaculture-derived organic matter in the sediment in and around a coastal fish farm using stable carbon and nitrogen isotope ratios. Aquaculture 254, 411–425. doi:10.1016/j.aquaculture.2005.10.024

Table 1
Click here to download Table: Dang et al. Table 1.docx

Table 1: Concentration in OC, N, P, C/N ratio and C, N isotope composition in river particles, surface sediments and sediments core collected from Toulon Bay.

Stations	{OC} in % (n)	{N} in % (n)	C/N (g g^{-1})	$\delta^{13}C$ (‰)	$\delta^{15}N$ (‰)	{P} in g g^{-1} (n)	
Las river particles	0.9 ± 0.6 (5)	0.07 ± 0.04 (5)	14.5 ± 2	-28.5±0.8	5.0±0.9	410 ± 145 (5)	
Eygoutier river particles	3.0 ± 1.2 (5)	0.21 ± 0.09 (5)	13.7 ± 0.9			1240 ± 360 (5)	
Surface sediments	3.9 ± 1.5 (59)	0.11 ± 0.07 (9)	17.5 ± 3.5	-24.5 to -19.8	0.5 to 4.5	530 ± 150 (59)[a]	
MIS	4.9 ± 1.3 (4)	0.25 ± 0.06 (4)	19.4 ± 3.9	-25.5±1.1	4.0±0.8	850[b]	1200± 350 (20)[c]
LAS1	2.2 ± 0.6 (20)	0.12 ± 0.03 (20)	18.9 ± 1.8	-28.6±0.6	1.4 to 2.8	2500[b]	550± 90 (12)[c]
LAS2	2.5 ± 1.1 (25)	0.21 ± 0.14 (25)	14.5 ± 4.6	-26.4±1.4	3.0±0.6	350[b]	370± 60 (18)[c]
3B	5.3 ± 1.2 (23)	0.24 ± 0.04 (5)	18.6 ± 2	-21.5±0.6	4.8 to 8.9	1100[b]	870± 90 (16)[c]
12	4.9 ± 0.6 (29)	0.24 ± 0.02 (5)	18.6 ± 1	-18.6±1.7	2.6 to 5.1	860[b]	450± 40 (22)[c]
15	6.8 ± 1.1 (28)	0.24 ± 0.03 (8)	21.1 ± 2.3	-16.8±1.7	1.7 to 4.9	760[b]	320± 33 (21)[c]
23	3.5 ± 0.6 (5)	0.12 ± 0.02 (5)	28.1 ± 3.2	-17.9±0.7	1.8±0.2	500[b]	300± 40 (13)[c]
52	1.3 ± 1 (4)	0.08 ± 0.04 (4)	17.8 ± 4.4	-22.6±0.6	0.2 to 1.9	540[b]	360± 30 (14)[c]

[a] 0-5 cm; [b] 0-2cm; [c] -15 cm to sediment core bottom

TABLES

Table 1: Concentration in OC, N, P, C/N ratio and C, N isotope composition in river particles, surface sediments and sediments core collected from Toulon Bay.

FIGURES

Figure 1: Map of the study site showing main anthropogenic activities. Las and Eygoutier Rivers are discharging into little and large Bay, respectively. Two treated sewage submarine outlets discharge into large Bay. Cross symbols show the location of 54 surface sediments while circle symbols locate eight sediment cores. The numbers adjacent to cross symbols correspond to the surface sediment samples where C and N isotope compositions are analyzed.

Figure 2: Concentration in organic Carbon and total P in surface sediments (0-5 cm) of Toulon Bay.

Figure 3: Biplot of the relationship between C, N, and P in river particles and sediments of Toulon Bay. The OC/N relationship in Station-12 porewater is reported by Dang et al. (2014a).

Figure 4: Biplot of C and N isotope composition in rivers particles, surface and core sediments. The three area plots show data reported from the literature for freshwater phytoplankton (yellow), estuarine-marine phytoplankton (blue) and seagrasses/macroalgae (green). Refer to Figure S4 and Table S1 for more details. The black circles summarize the five potential sources used in the IsoSource program, while the grey circle positions the isotopic composition revealed in a wetland (Li et al., 2016).

Figure 5: Comparison of the modeled and observed C and N isotope composition by the multiple end-member mixing model. In the panel B, the symbol size is proportional to the contribution of Source4, the full line shows the regression passing through zero while the dashed line shows the regression line fitting the data.

Figure 6: Radar plots showing contributions of five sources at six sediment cores. Line-and-scatter plots show the average of the whole sediment core while line plots show the minimal and maximal values.

Figure 7: Total P vs. $\delta^{15}N$; black circles show the relationship between total P and N isotope composition in bulk sediments. Colored symbols represent individual sediment cores while

comparing total P to anthropogenic N isotope composition with the relationship of $P = 270 \times \delta^{15}N_{anthr.} + 415$.

Figure 8: Comparison of total P to Iodine and Mg in surface sediments and sediment cores. Correlations are only observed for stations 15, 23 and 52.

Figure 9: Map of anthropogenic P loading in the Toulon Bay revealing non-point source (northern Little Bay) and point sources (aquaculture: station 15 and treated sewage: stations 39 and 42).

Figure 10: Estimated non-anthropogenic (diagenetic) P profiles at six stations (A) and the averaged profile (B). The non-anthropogenic P background is represented by the vertical red line and the variation range in total P of six sediment cores is shown by the grey zone in (B). Refer to Figure S2 for individual total P profiles.

Figure 1
Click here to download high resolution image

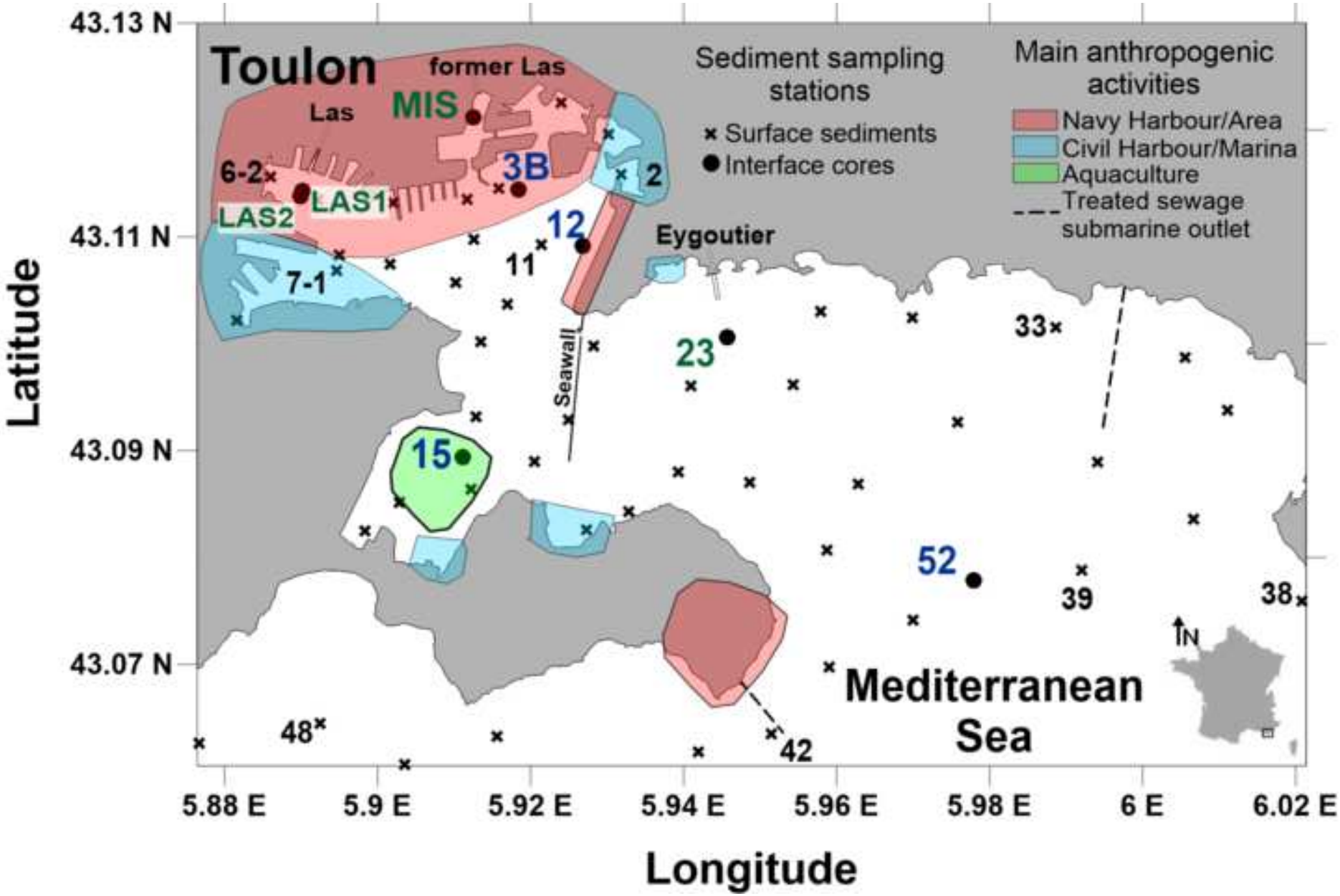

Figure 2
Click here to download high resolution image

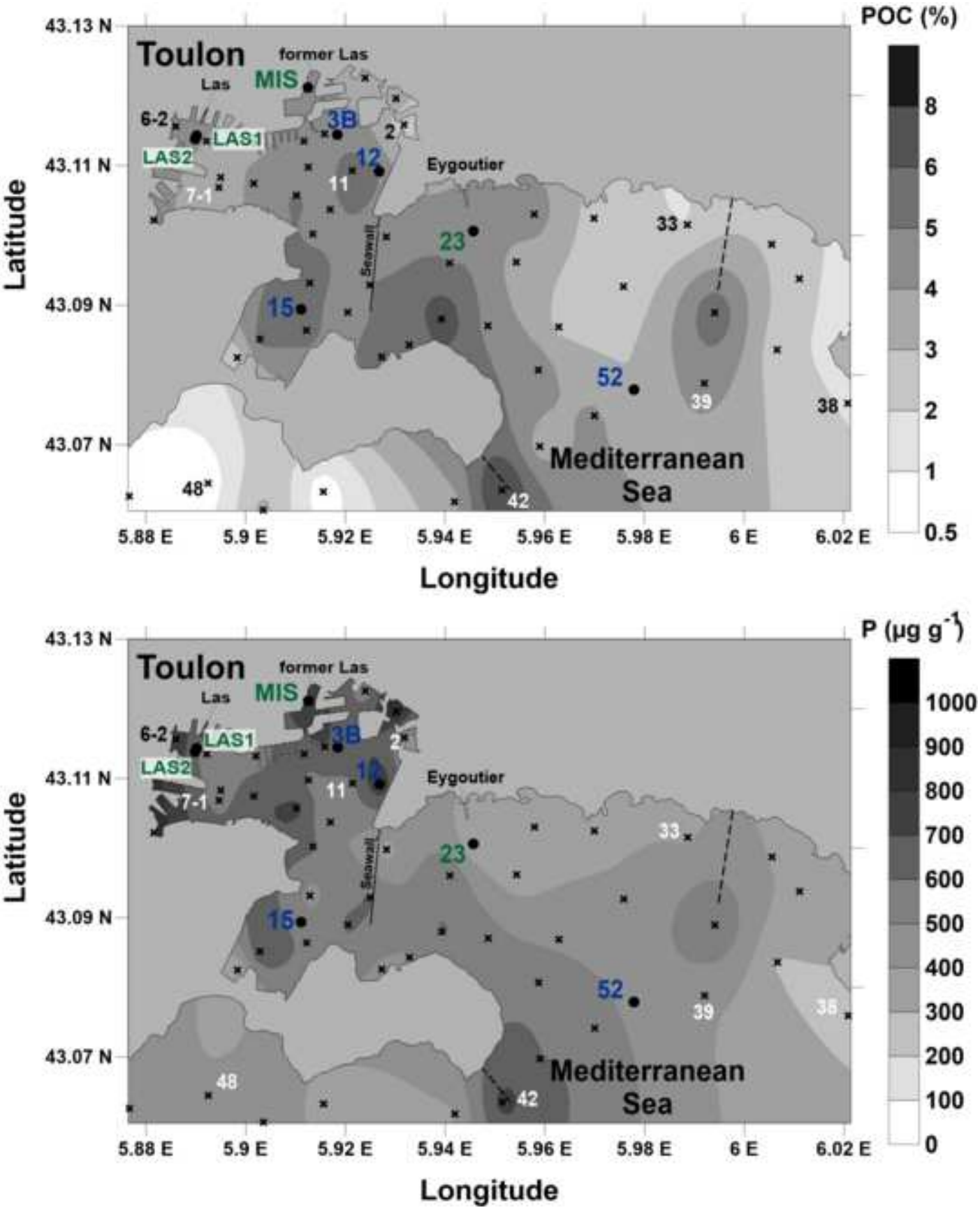

Figure 3
Click here to download high resolution image

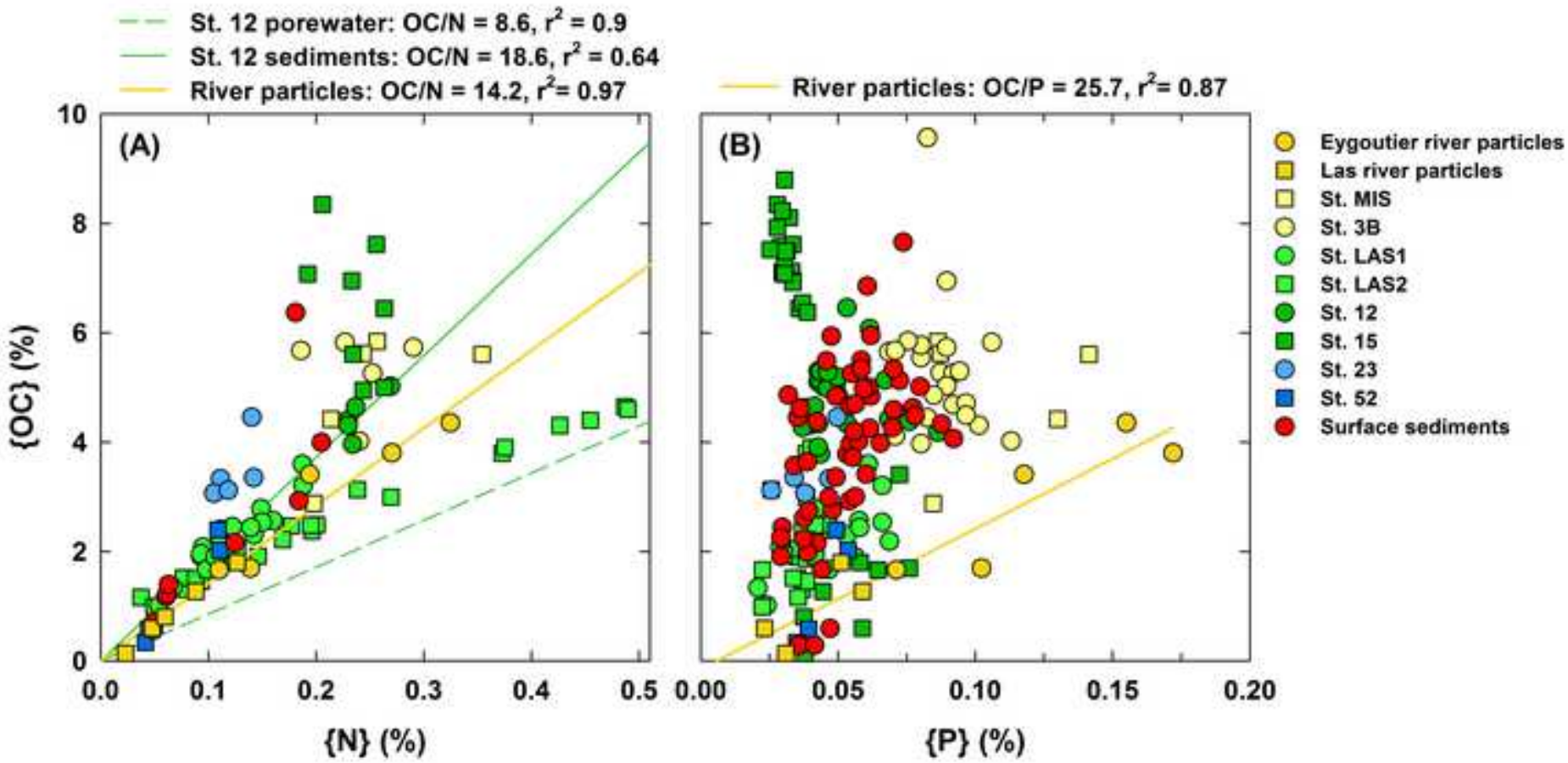

Figure 4
Click here to download high resolution image

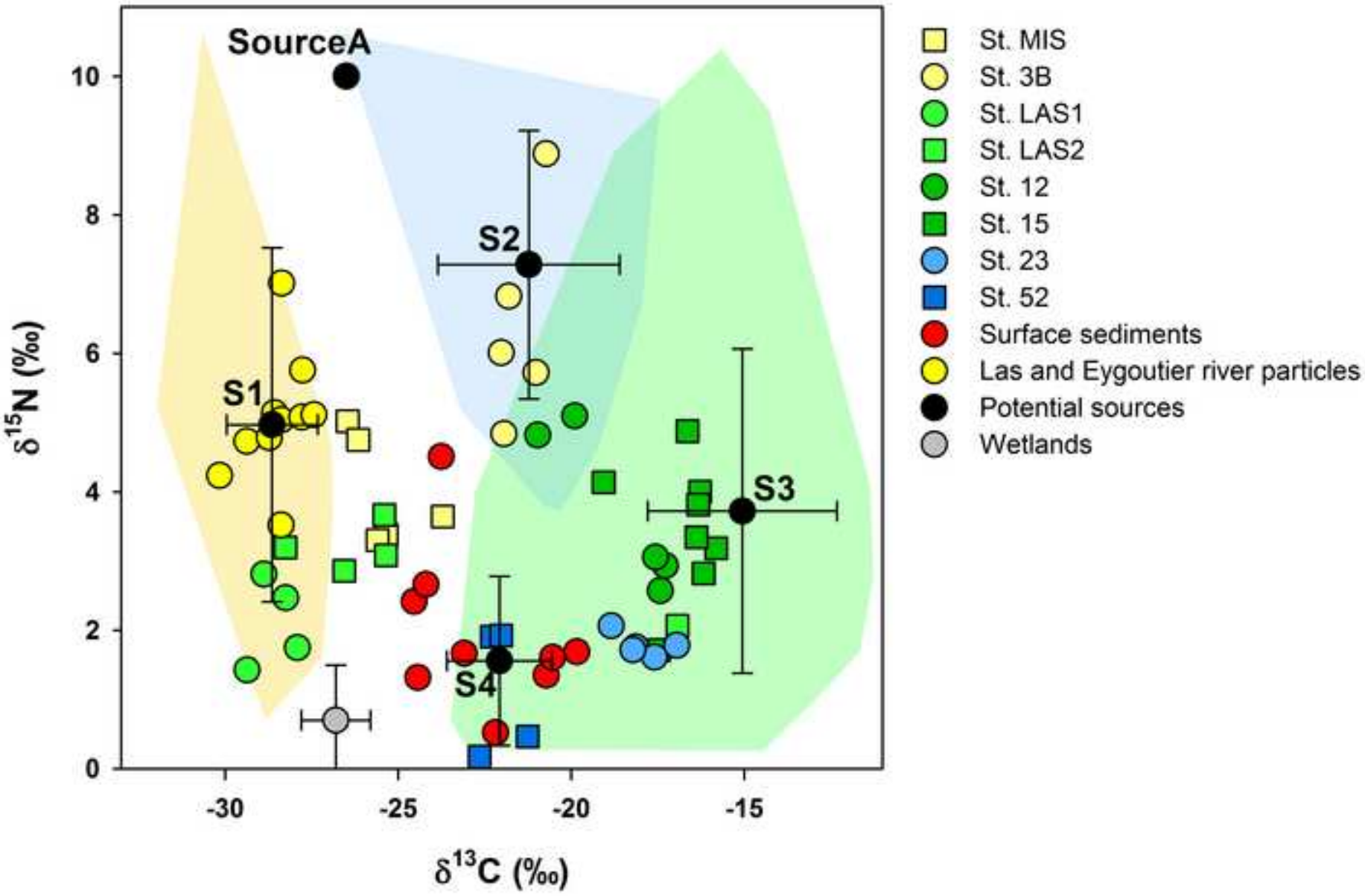

Figure 5
Click here to download high resolution image

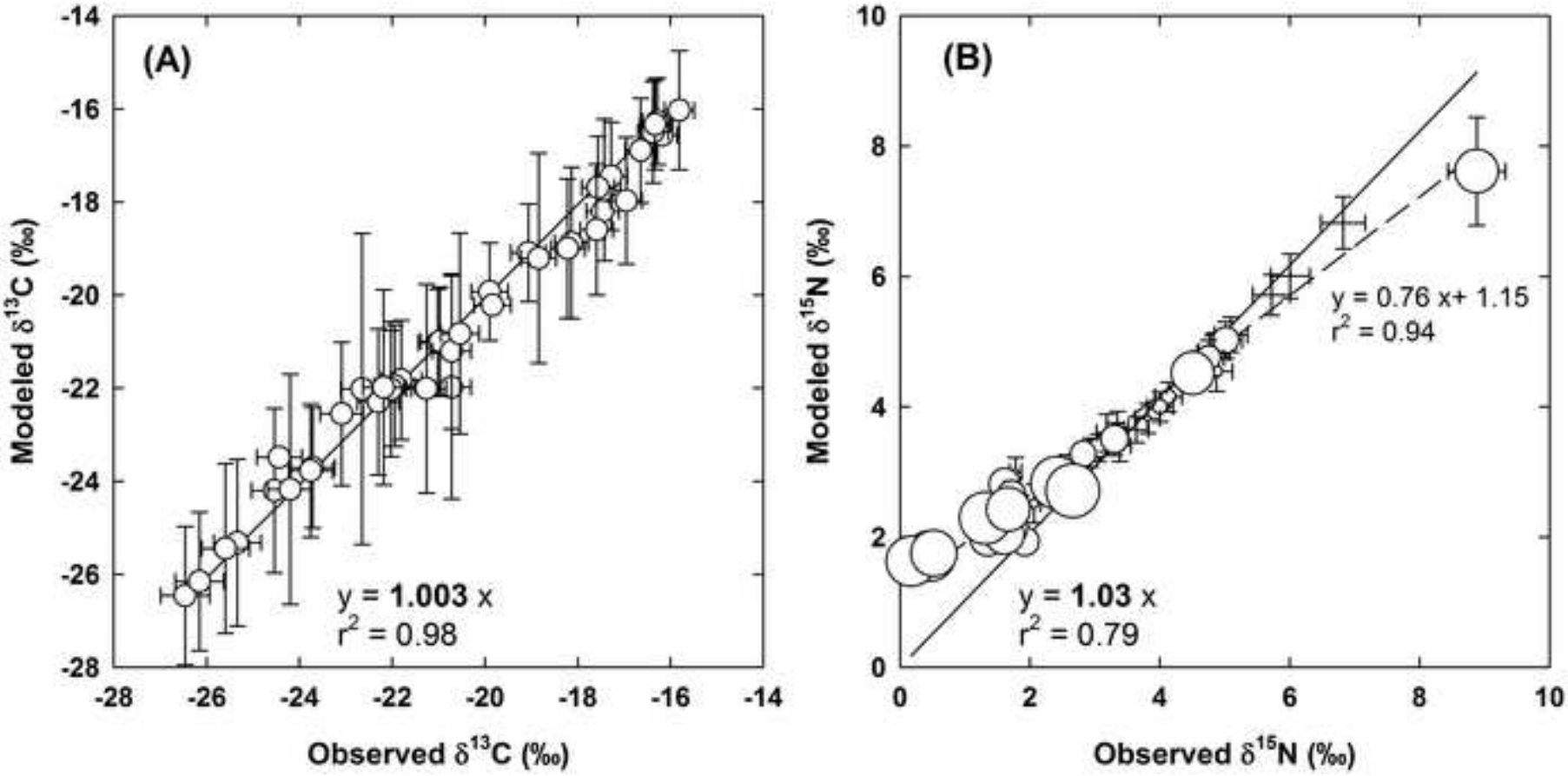

Figure 6

Click here to download high resolution image

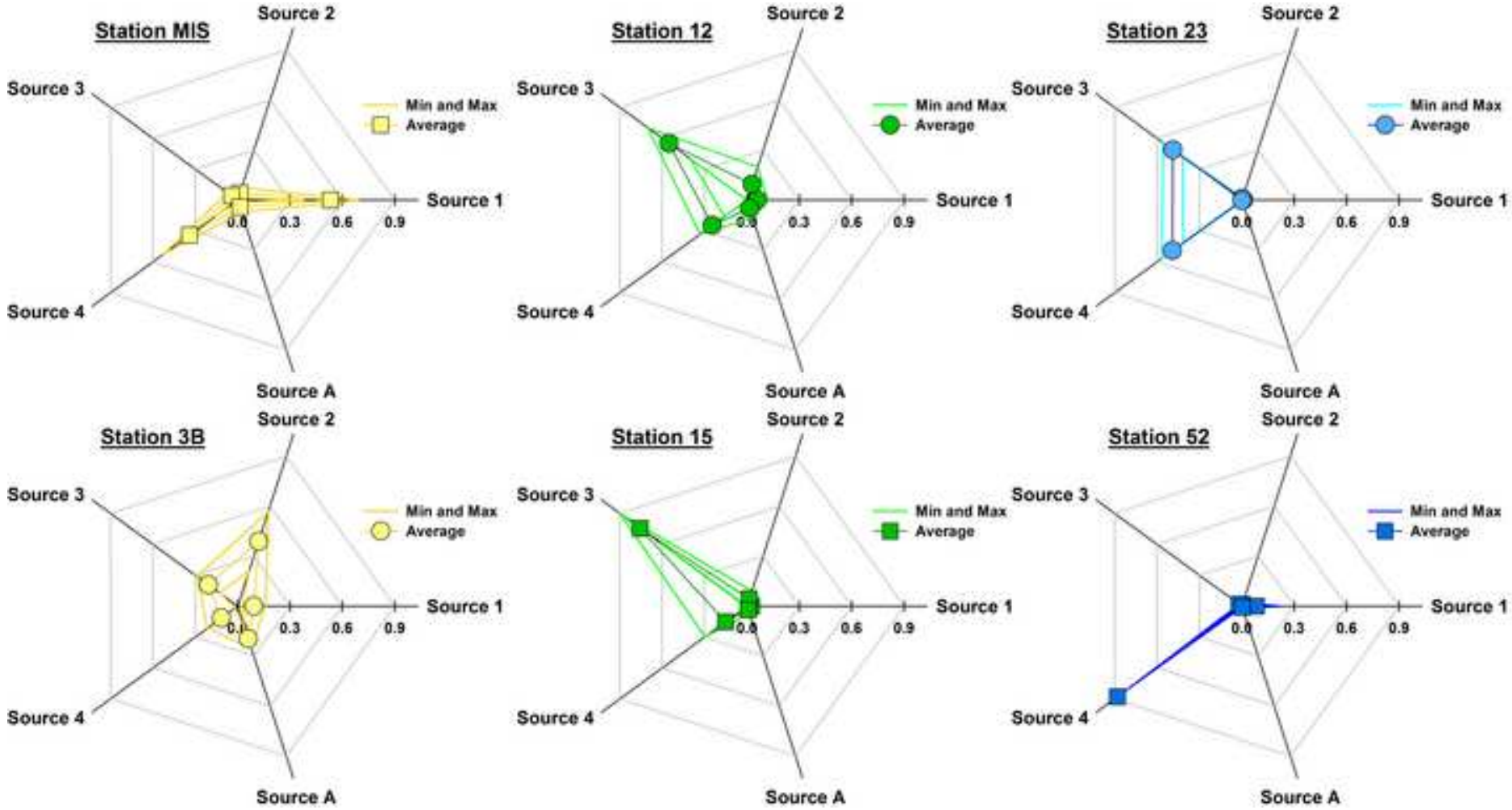

Figure 7
Click here to download high resolution image

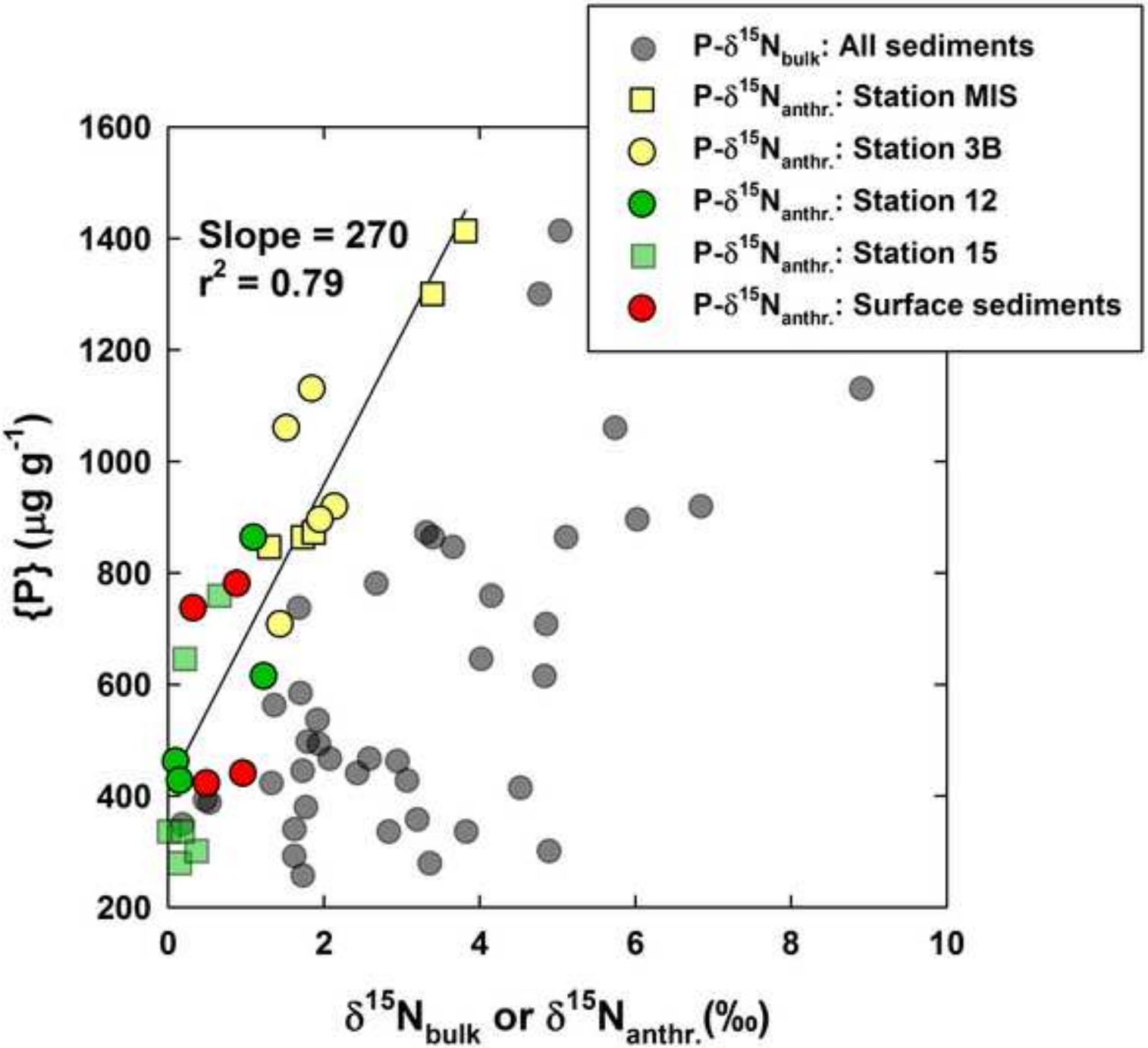

Figure 8
Click here to download high resolution image

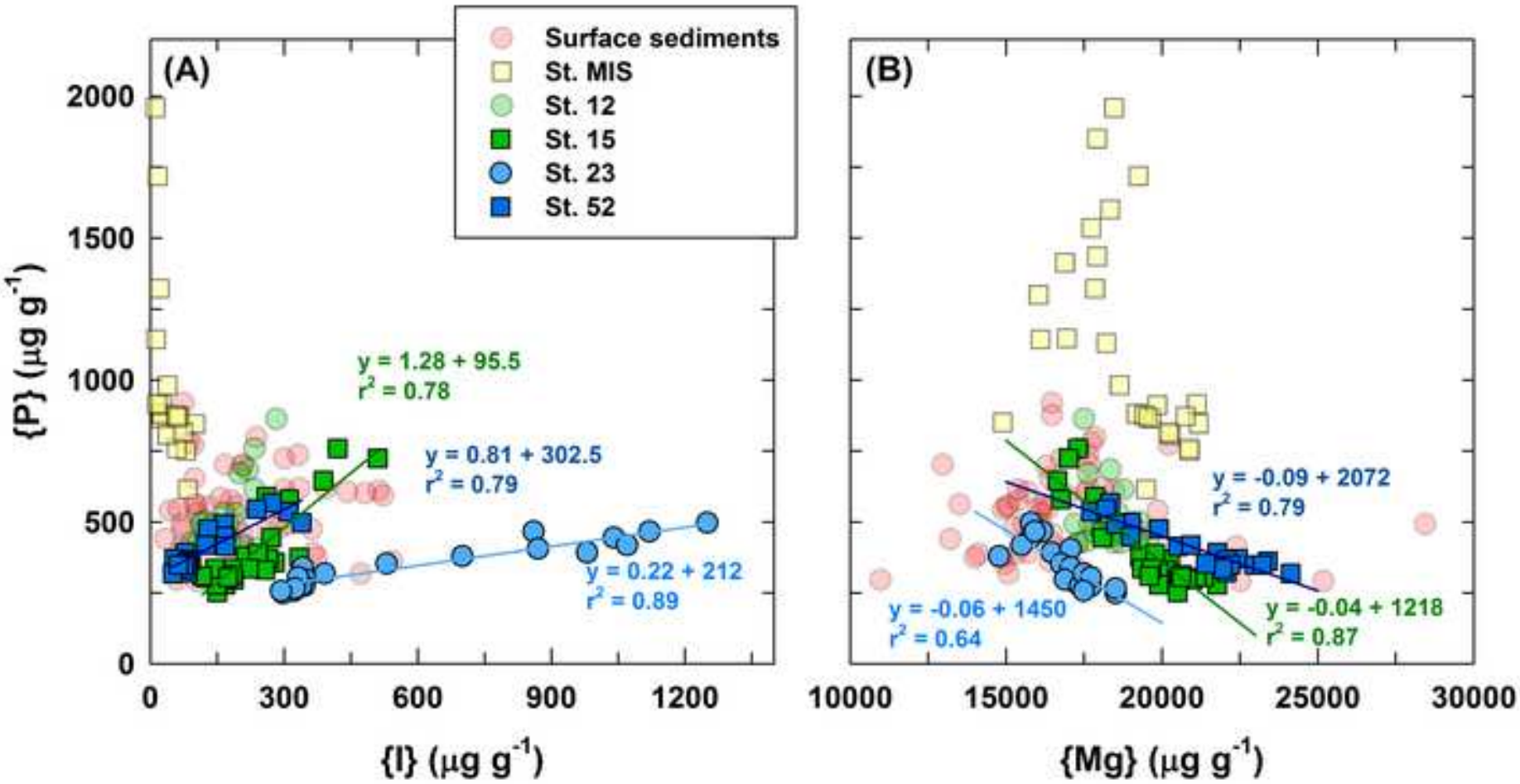

Figure 9
Click here to download high resolution image

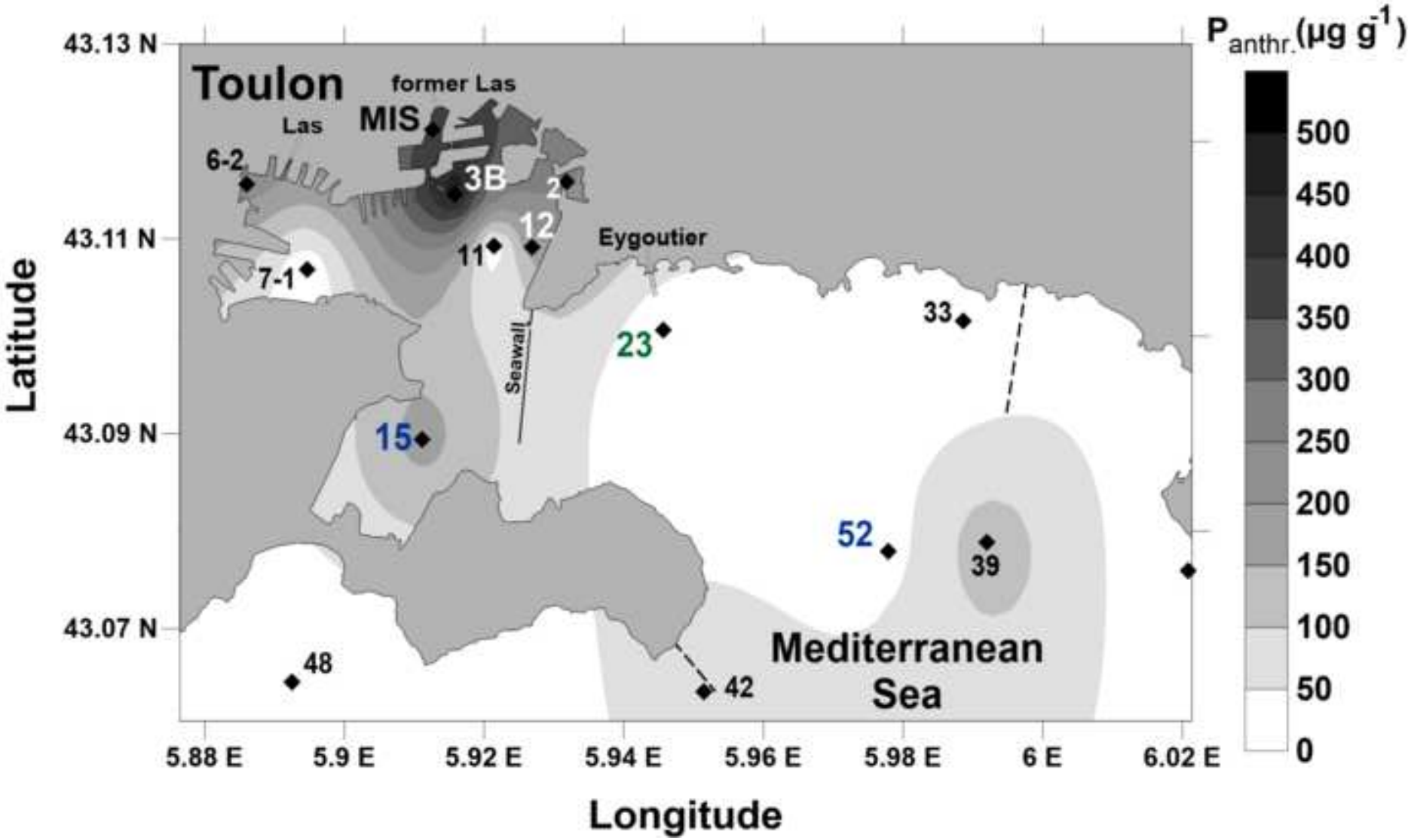

Figure 10
Click here to download high resolution image

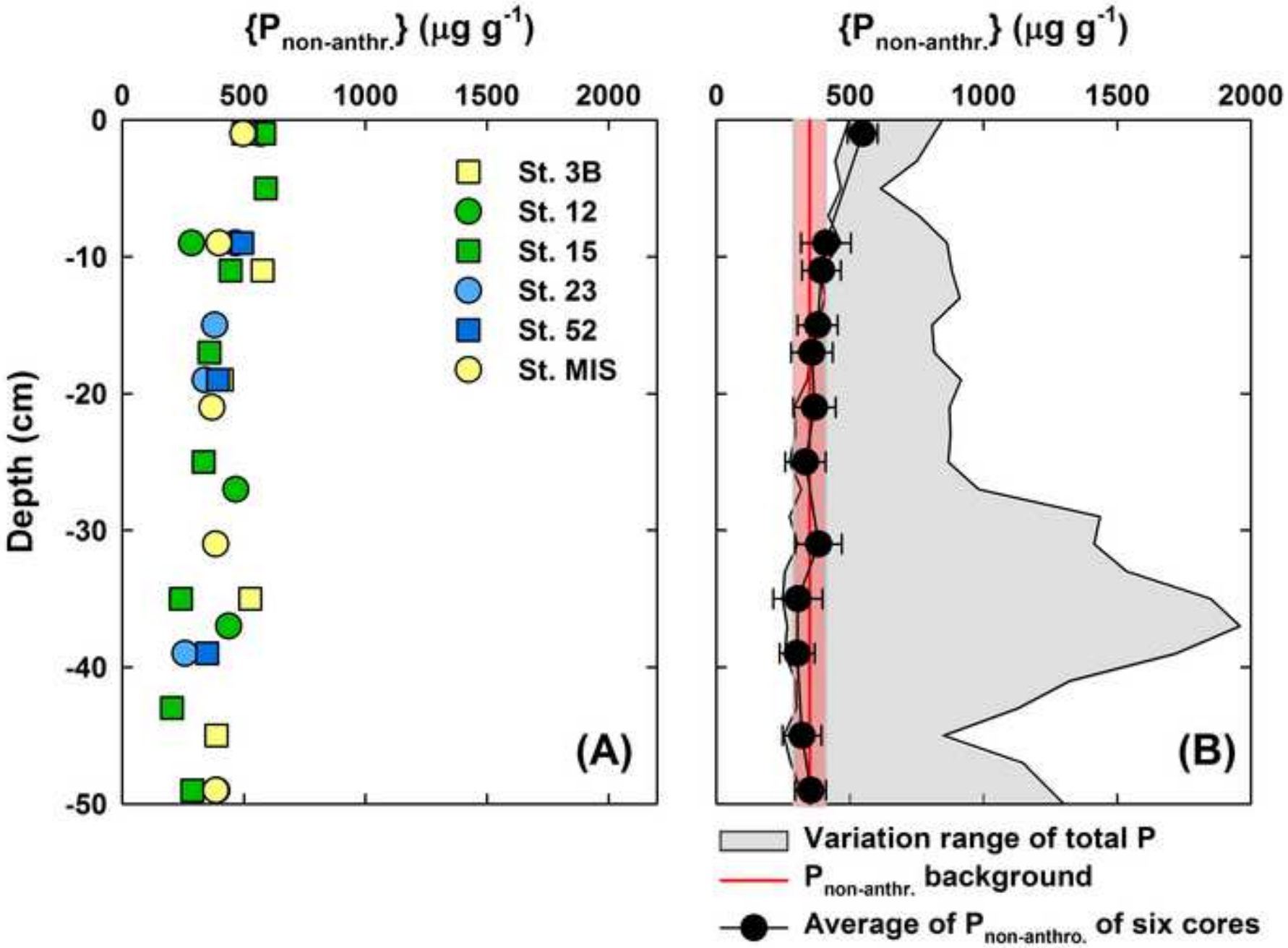

Electronic Supplementary Material (for online publication only)
Click here to download Electronic Supplementary Material (for online publication only): Dang et al. Supplementary information.p